Multinuclear NMR Studies on Al(III) Complexes of ATP and Related Compounds

S. J. Karlik, G. A. Elgavish,[1] and G. L. Eichhorn*

Contribution from the National Institutes of Health, National Institute on Aging, Gerontology Research Center, Baltimore, Maryland 21224. *Received May 10, 1982*

Abstract: The NMR spectra of Al(III) complexes of ATP, using ^{27}Al, ^{31}P, and ^{1}H nuclei, frequently exhibit slow-exchange features and can be used directly to study the characteristics of the complexes. The resolution of the ^{27}Al peaks at low pH makes possible affinity calculations that show, e.g., that 97% of the Al(III) is bound to ATP at pH 2. Al(III) complexation generally leads to upfield shifts of the ^{31}P peaks of ATP, as well as AMP, ADP, NADP, GMP, GDP, dATP, GTP and ortho-, pyro-, and triphosphate; occasional downfield shifts are also noted. The ^{1}H peaks of ATP are also generally upfield shifted. The combination of all the NMR results indicates that Al(III) forms at least four complexes with ATP, that there is generally more than one complex present under any set of conditions, and that the equilibria between these complexes shift dramatically with pH. Al(III) has no effect on the ^{1}H spectrum of adenosine, but it has some very similar effects on the ^{31}P spectra of triphosphate and ATP. The following Al(III)–ATP complexes have been identified, in the order of appearance with increasing pH: (1) Al(III) bound to β- and γ-phosphates, with no effect on the bases, (2) Al(III) bound to γ-phosphate and N-7 (β-phosphate binding not certain), (3) Al(III) bound to β- and γ-phosphates, and the bases stacked, and (4) Al(III) bound only to γ-phosphates. Rates of exchange between these complexes have been calculated; they are in the range characteristic of aluminum complexes.

The interaction of aluminum with cellular components has recently aroused interest because Al has been implicated in a number of toxic biological processes, among them the accumulation of Al(III) in localized areas of brain in Alzheimer's disease[2] and the toxicity due to Al(III) produced in the course of lengthy kidney dialysis treatment leading to dialysis dementia.[3] In the latter ailment the toxic effects of Al(III) have been thought to be due to the binding of Al(III) to ATP and the consequent inhibition of reactions that require ATP participation.[4] For this reason the complexes formed between ATP and Al(III) are of some significance.

The reactions of aluminum in aqueous solution are complicated by the fact that Al(III) exists in a variety of species, whose relative concentration depends on the degree of binding of OH^- groups and therefore on the pH.[5] We have therefore studied Al(III) binding to ATP as a function of pH, using ^{27}Al, ^{31}P, and ^{1}H NMR. Similar studies were carried out with aluminum complexes of AMP, ADP, NADP, GMP, GDP, dATP, GTP, and ortho-, pyro-, and triphosphate;[6] a comparison of the NMR spectra of these complexes with those of ATP has proved helpful in the determination of various aspects of the structures of the Al–ATP complexes.

This work has demonstrated a rather extraordinary degree of binding of Al(III) to ATP at the extremes of pH, unusually good resolution of the peaks of complexed and uncomplexed ligand due to slow exchange, and a complicated series of equilibria between at least four complexes of Al(III) and ATP. Many features of the structures of these complexes have been worked out.

Most of the experiments have been conducted under conditions that promote the formation of 1:1 Al–ligand complexes and not complexes that contain more ligand than Al(III). In this way these complex equilibria are at least simplified to the extent that complexes with stoichiometries other than 1:1 are avoided. Some evidence from studies with excess ligand also indicates that the 1:1 complexes are preferred anyway.

The Cr(III) and Co(III) complexes of ATP have been studied extensively by Cleland et al.[7] The structural features of these trivalent metal complexes can therefore be compared with those of the Al(III) complexes.

Experimental Section

Materials. Adenosine 5′-triphosphate (ATP) was purchased from Sigma Chemical and passed through pretreated Chelex resin (Bio-Rad). The $AlCl_3$ stock was prepared from 99.9995% $AlCl_3 \cdot 6H_2O$ (Gallard–Schlesinger). This high-quality aluminum salt was employed to minimize paramagnetic contamination; final concentration of paramagnetic ions was thus <0.05 ppm. Other phosphate compounds were purchased from Sigma (AMP, dATP, UTP, GMP, NADPH, ADP), PL Biochemicals (GTP, ADP, CDP), Calbiochem (NADPH),[6] Fisher (sodium pyrophosphate, TP), and J. T. Baker (sodium dihydrogen phosphate) and used without further treatment.

Methods. The products obtained by mixing aluminum salts with various ligands are dependent on the order of mixing; long-lived metastable complexes have been observed.[8] In the studies reported here, all compounds were added to the aluminum solution at pH 1; thus aluminum was temporarily in excess during mixing. pH values were obtained on a Radiometer PMH pH meter equipped with a 3-mm electrode (Wilmad). All pHs were adjusted to ±0.05 unit from the reported value; pH values in D_2O solutions were corrected for the deuterium isotope effect by adding 0.4 to the meter reading.

Nuclear Magnetic Resonance Experiments. ^{27}Al, ^{31}P, and ^{1}H NMR spectra were recorded at 21–22 °C on a Varian XL-200 spectrometer at 52.1, 81.0, and 200.0 MHz, respectively. The aluminum and phosphorus spectra in aqueous solution were obtained with a tunable broad-band probe in 10-mm tubes; a fixed frequency probe was used for proton spectra in D_2O with 5-mm tubes. External 100 mM $AlCl_3$ (pH 1) and 85% orthophosphoric acid and internal 2-methyl-2-propanol were employed as standards; all downfield shifts are reported as positive values. D_2O employed for lock was contained in a 4-mm internal tube for the ^{27}Al and ^{31}P samples.

The ^{31}P and ^{1}H peak intensities were measured by tracing, cutting out, and weighing expanded spectra or by an automatic spectrometer routine.

(1) Current address: Comprehensive Cancer Center, University of Alabama in Birmingham, Birmingham, AL 35294.

(2) (a) Crapper, D. R.; Krishnan, S. S.; Dalton, A. J. *Science (Washington, D.C.)* **1973**, *180*, 511. (b) Crapper, D. R.; Karlik, S. J.; DeBoni, U. *Aging (N.Y.)* **1978**, *7*, 471. (c) Crapper, D. R.; Quittkat, S.; Krishnan, S. S.; Dalton, A. J.; DeBoni, U. *Acta Neuropathol.* **1980**, *50*, 19. (d) Perl, D. P.; Brody, A. R. *Science (Washington, D.C.)* **1980**, *208*, 297.

(3) (a) Alfrey, A. C.; LeGendre, G. R.; Kaehny, W. D. *N. Engl. J. Med.* **1976**, *294*, 184. (b) Arieff, A. I.; Cooper, J.; Armstrong, D.; Lazaromitz, V. C. *Ann. Intern. Med.* **1979**, *90*, 741. (c) Kovalchik, M. T.; Kaehny, W. D.; Hegg, A. P.; Jackson, J. T.; Alfrey, A. C. *J. Lab. Clin. Med.* **1978**, *92*, 712.

(4) (a) Womack, F. C.; Colowick, S. P. *Proc. Natl. Acad. Sci. U.S.A.* **1979**, *76*, 5080. (b) Solheim, L. P.; Fromm, H. J. *Biochemistry* **1980**, *19*, 6074. (c) Solheim, L. P.; Fromm, H. J. *Anal. Biochem.* **1980**, *109*, 266. (d) Viola, R. E.; Morrison, J. F.; Cleland, W. W. *Biochemistry* **1980**, *19*, 3131.

(5) Baes, C. F.; Messmer, R. E. "The Hydrolysis of Cations"; Wiley: New York, 1976.

(6) Abbreviations used: AMP, adenosine 5′- monophosphate; ADP, adenosine 5′-diphosphate; NADP, nicotinamide adenine dinucleotide 2′-phosphate; GMP, guanosine 5′-monophosphate; GDP, guanosine 5′-diphosphate; dATP, deoxyadenosine 5′-triphosphate; GTP, guanosine 5-triphosphate; TP, triphosphate.

(7) (a) DePamphilis, M. L.; Cleland, W. W. *Biochemistry* **1973**, *12*, 3714. (b) Janson, C.; Cleland, W. W. *J. Biol. Chem.* **1974**, *249*, 2562. (c) *Ibid.* **1974**, *249*, 2567. (d) *Ibid.* **1974**, *249*, 2572. (e) Cornelius, R.; Hart, P.; Cleland, W. W. *Inorg. Chem.* **1977**, *16*, 2799. (f) Cornelius, R.; Cleland, W. W. *Biochemistry* **1978**, *17*, 3279. (g) Raushel, F.; Cleland, W. W. *Ibid.* **1977**, *16*, 2169. (h) Merritt, E.; Sunderalingam, M.; Cornelius, R.; Cleland, W. W. *Ibid.* **1978**, *17*, 3274. (i) Dunaway-Mariano, D.; Cleland, W. W. *Ibid.* **1980**, *19*, 1496.

(8) Karlik, S. J.; Tarien, E.; Elgavish, G.; Eichhorn, G. L. *Inorg. Chem.*, in press.

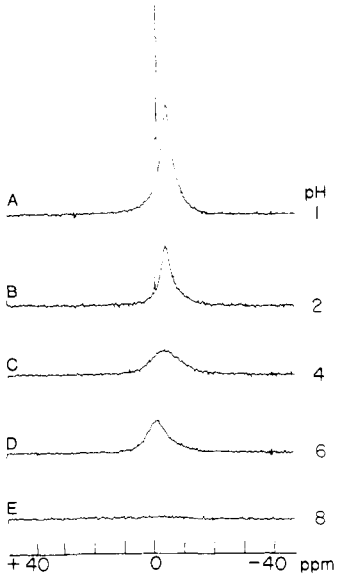

Figure 1. ^{27}Al NMR spectra (52.13 MHz, 22 °C) of 10 mM $AlCl_3$–10 mM ATP solutions mixed at pH 1 (A) and increased to pH 2 (B), 4 (C), 6 (D), and 8 (E). Spectra were obtained with a spectral width of 10 000 Hz, acquisition time 0.5 s, line broadening 1 Hz, 90° pulse width 12 μs, number of scans 2000, 0 ppm at $Al(H_2O)_6^{3+}$.

Where overlapping occurred, the area of an individual resonance was estimated visually. The overall error was estimated to be 15% throughout six experiments. Integration of less complex ^{27}Al intensities was performed by the automatic spectrometer routine. Nonsaturating conditions were estabished by increasing the acquisition time for all NMR nuclei until the signals reached constant intensity.

Results

Aluminum-27 Spectra. The ^{27}Al spectrum of the Al–ATP complex illustrates the rather remarkable slow-exchange properties of NMR spectra of some Al(III) complexes. Al(III) binding to ATP produces shifts upfield from $Al(H_2O)_6^{3+}$ in the ^{27}Al spectrum as illustrated in Figure 1 for 1:1 Al–ATP mixtures. The upfield shift is consistent with the ^{27}Al NMR shifts observed for Al(III) complexes with phosphoric acid,[9] trimethyl phosphate,[10] and a variety of phosphate-containing ligands.[11] The upfield shift produced for phosphate and sulfate ligands contrasts with the downfield shifts observed for most other ligands in aqueous solution.[12]

Two separate peaks can be observed at low pH; a sharp line corresponding to $Al(H_2O)_6^{3+}$ and a broad peak 3 ppm upfield, representing the complex of aluminum with ATP (Figure 1, A and B). From the relative areas of these peaks at pH 1, 1.5 (not shown), and 2, the fraction of aluminum bound to ATP was calculated to be 79, 89, and 97%, respectively; corresponding association constants at these pH values were calculated to be 1800, 7400, and 110 000 M^{-1}. At pH 4 (Figure 1C), the disappearance of the $Al(H_2O)_6^{3+}$ line is accompanied by a 1 ppm downfield shift of the Al–ATP peak from its position at pH 1. At pH 6 (Figure 1D), this peak has moved 1 ppm further downfield and is sharpened. This resonance is then progressively broadened by further increase in pH; at pH 8, the ^{27}Al–NMR signal is not detectable (Figure 1E).

At low pH (1–2), therefore, aluminum is in slow exchange on the ^{27}Al NMR chemical shift time scale between the hexaaquo and ATP-bound forms. Increasing the pH increases the fraction of aluminum bound to ATP, and above pH 4 the $Al(H_2O)_6^{3+}$ concentration is too low to be observed by NMR. The peak corresponding to ATP-bound aluminum is shifted downfield with increasing pH and broadens at pH >6. Downfield shifts and line broadening with increasing pH may be attributed to hydroxide ion participation in the aluminum–ligand field in reactions that exhibit fast exchange. Because the aluminum nucleus is quadrupolar, asymmetry in the ligand field produces an increase in the NMR line width. Thus, ligand substitution by a variable number of hydroxides can yield a variety of nonsymmetric aluminum environments with increased ^{27}Al NMR line widths. This phenomenon has also been observed for complexes of aluminum with carboxyl ligands.[8]

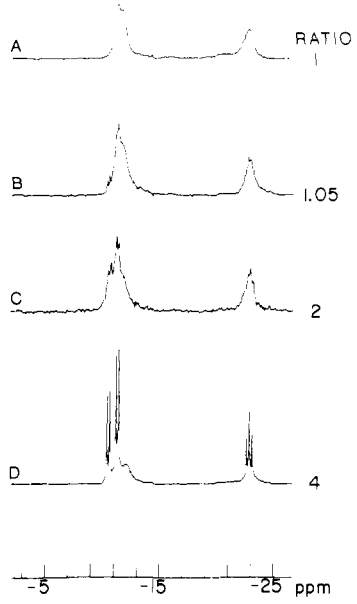

Figure 2. ^{31}P NMR spectra (80.98 MHz, 22 °C) of aluminum–ATP mixture at pH 5. Spectrum (A) was obtained by mixing an equal volume of ATP into $AlCl_3$ at pH 1 followed by adjusting the pH to 5. ATP (pH 5) was added to yield the following ATP/Al ratios: 1.05 (B), 2 (C), 4 (D). Spectra were obtained with a spectral width of 3000 Hz, acquisition time 1.6 s, line broadening 2 Hz, 90° pulse width 16.0 μs, 400 scans.

Although a pH-induced broadening suggests increased hydroxide participation, it is not possible with ^{27}Al NMR to distinguish whether an increase in hydroxylation results in dissociation of the Al–ATP complex, because the ligand-field alteration may produce broadening whether or not phosphate continues to occupy coodination sites.

Phosphorus-31 Spectra. A. Al and ATP. Analysis of the ^{31}P spectrum of Al–ATP complexes leads, first of all, to evidence that 1:1 Al–ligand complexes predominate. The spectrum of an equimolar solution of $AlCl_3$ and ATP (10 mM each) at pH 5 (Figure 2A) contains only two broad resonances. As the ATP concentration is increased beyond the 1:1 ratio of ATP/Al, relatively sharp resonance lines (~5–7-Hz width) are observed, superimposed on the two broad peaks (Figure 2, B–D). The chemical shifts of these sharp peaks are identical with those of ATP resonances in the absence of aluminum. The intensity of these free ATP resonances increases with increasing ATP/Al ratio while the broad resonances, which must be those for aluminum-bound ATP, remain unchanged. We conclude that the exchange between bound and free ATP is also slow on the ^{31}P NMR chemical shift time scale and that Al tends to bind to only one molecule of ATP. With the exception of the experiment shown in Figure 2, all experimental solutions contain a 1:1 ratio of Al to ATP.

An examination of ^{31}P spectra at various pHs (Figure 3) reveals that a number of complexes exist and that the equilibrium between these is greatly affected by pH, as may be expected. At pH 1, the spectrum consists of peaks at ~−12, −15, −21, −23, and −27 ppm (Figure 3A). The strong binding of aluminum to ATP indicated by the ^{27}Al spectrum at pH as low as 1 (Figure 1A) is confirmed by ^{31}P NMR. The spectrum at pH 2 is similar to that at pH 1, but the peak intensities are altered (Figure 3B). An

(9) Akitt, J. W.; Greenwood, N. W.; Lester, G. D. *J. Chem. Soc. A* **1971**, 2450.
(10) Delpuech, J. J.; Khadder, M. R.; Peguy, A.; Rubini, P. *J. Am. Chem. Soc.* **1975**, *97*, 3373.
(11) Karlik, S. J.; Elgavish, G.; Pillai, R. P.; Eichhorn, G. L. *J. Magn. Reson.* **1982**, *49*, 164.
(12) Akitt, J. W. *Annu. Rep. NMR Spectrosc.* **1972**, *5A*, 465.

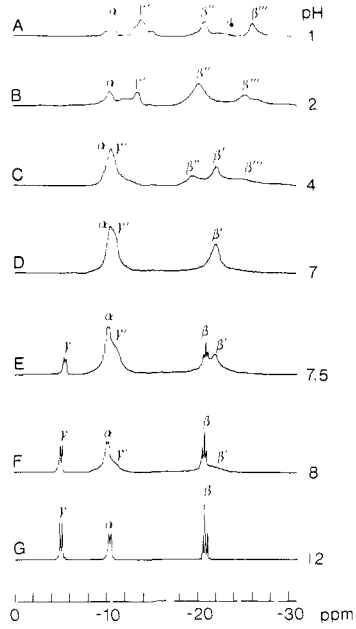

Figure 3. ^{31}P NMR spectra of 10 mM $AlCl_3$ and ATP at pH 1 (A) and increased to pH 2 (B), 4 (C), 7 (D), 7.5 (E), 8 (F), and 12 (G), conditions as in Figure 1. See Discussion for assignments of γ', β', β'', and β''' resonances that appear in the presence of aluminum.

equimolar mixture of Al and ATP is not soluble between pH ~2.5 and 3.5.

Four broad peaks are observed at pH 4 (Figure 3C) because of the merger of two peaks observed at lower pH. Resonances at −19 and −25 ppm correspond to those also observed at pH 1 and 2, although they are shifted downfield 2 ppm and exhibit a reduced intensity; these peaks are lost at higher pH. The peaks at −11 and −22 ppm (Figure 3C) remain relatively unshifted through further pH increases (Figure 3, D and E). Above pH 7, sharp resonances (5–7-Hz line width) appear in the Al–ATP spectra (Figure 3, E and F), corresponding to those of ATP in the absence of aluminum at the same pH. The increase in uncomplexed ATP in the ^{31}P NMR spectra reveals the onset of dissociation of the Al–ATP species.

B. Aluminum and Other Phosphate Ligands. In order to be able to interpret the perturbations caused by Al^{3+} on the ^{31}P NMR resonances of ATP, we examined the effect of aluminum on a number of other phosphate-containing compounds. These experiments were carried out at low pH with equimolar Al and ligand concentrations. In this pH range, the α- and β-phosphate signals of diphosphates and the α and γ signals of triphosphates are superimposed but, as we shall see, become separated on complexation.

Binding of aluminum to orthophosphate broadens the ^{31}P NMR signal and shifts it upfield 8.4, 12.4, and 17.6 ppm (Figure 4, A and B). The broadening and upfield shifts are observed when the aluminum is complexed with GMP and AMP and to the nonbridging phosphate of NADP (Figure 4, G and H).

When aluminum binds to a diphosphate, the resulting ^{31}P signals are also broadened and shifted upfield. The magnitude of the shift is 2.9 ppm for pyrophosphate and 2.8 and 3.5 ppm for ADP (Figure 4D) and 4.0, 7.6, and 14 ppm for the diphosphate bridge in NADP (Figure 4, G and H).

The effect of aluminum on triphosphate is still more complex. The ^{31}P spectrum of an equimolar mixture of aluminum with ATP (Figure 3A), GTP (Figure 4F), or triphosphate (TP) (Figure 5A) contains several broad peaks. One-half of the −11 ppm peak (Figure 4E), which corresponds to overlapping γ- and α-phosphate resonances, is shifted upfield (Figure 4F); the magnitude of the shift is the same as that observed for diphosphates. Only the unshifted peak at −11 ppm shows a net NOE when broad-band ^1H decoupling is applied; the peak therefore must be due to α-phosphate. Thus, the γ resonance is shifted upfield by aluminum, while the α resonance remains unshifted. Moreover, the

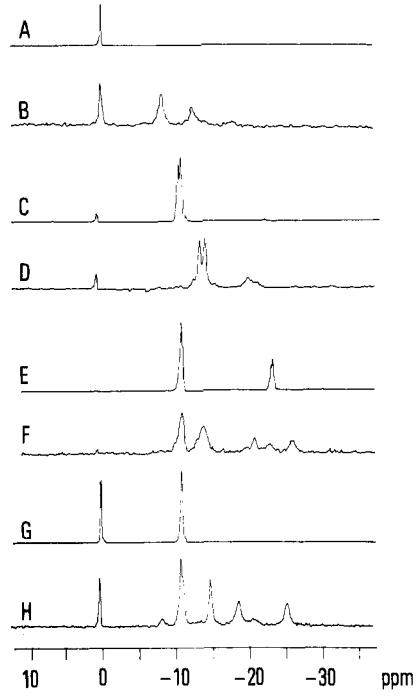

Figure 4. ^{31}P NMR spectra of Al complexes with phosphate-containing ligands at pH 2: (A) orthophosphate; (B) orthophosphate and aluminum; (C) ADP; (D) ADP and Al; (E) GTP; (F) GTP and Al; (G) NADP; (H) NADP and Al. NMR conditions as in Figure 2; Al and ligand concentrations were 10 mM each.

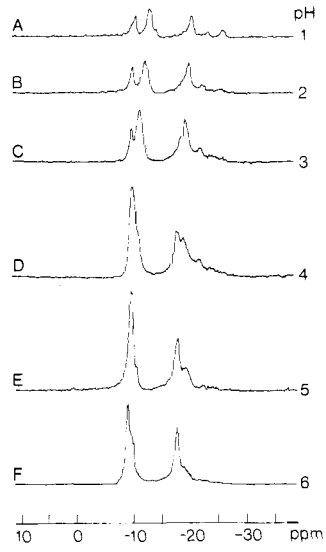

Figure 5. ^{31}P NMR spectra of 10 mM sodium triphosphate and 10 mM $AlCl_3$ mixed at pH 1 (A) and increased to pH 2 (B), 3 (C), 4 (D), 5 (E), and 6 (F). Conditions as in Figure 2.

β-phosphate at −24 ppm (Figure 4E) is split into three peaks, including *two* additional resonances at −21 and −27 ppm (Figure 4F).

The ^{31}P NMR spectra of an equimolar mixture of aluminum and triphosphate (TP) were examined more closely, in order to observe any similarities and differences from those of Al–ATP mixtures (Figure 3), by obtaining a pH profile between pH 1 and 6 (Figure 5). At pH 1, the spectra are remarkably similar and consist of five resonances in nearly the same chemical shift positions. It is indeed striking that chemical shift alterations produced by aluminum on ATP and GTP α- and γ-phosphates are very similar to those observed with TP. Although the α- and γ-(terminal) phosphates of TP are identical, only one of these is perturbed by the binding of Al between pH 1 and 3, in a manner identical with the behavior of ATP and GTP. Thus, binding to

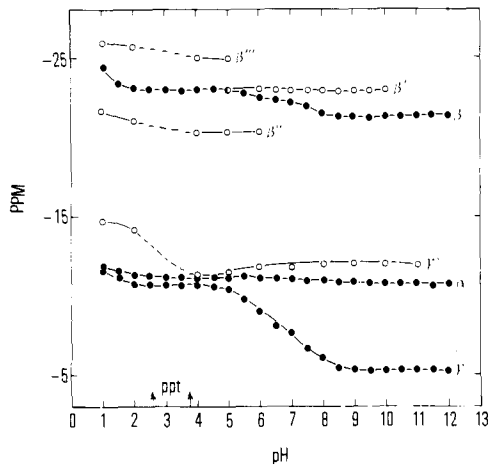

Figure 6. ^{31}P chemical shifts of the phosphate groups for 10 mM ATP in the absence (α, β, γ) and in the presence (γ', β', β'', β''') of 10 mM $AlCl_3$. See Discussion for assignment of γ', β', β'', and β''' resonances.

one phosphate in TP makes that phosphate resemble γ-phosphate in ATP and renders the other terminus inactive, like α-phosphate in ATP. As the pH is increased, the peak at −14 ppm (γ-like) moves downfield and merges with the peak at −10 ppm (α-like) at pH 4 (Figure 5B–D). This downfield shift probably reflects deprotonation of an aluminum-bound phosphate. The multiplicity of peaks observed for the center phosphate (corresponding to β) presumably reflects the formation of a number of complexes. As the pH approaches neutral, the TP spectrum again becomes virtually identical with the spectrum of ATP.

Thus, the effect of Al(III) on the ^{31}P NMR spectrum of phosphate ligands depends primarily on the number of phosphates within the ligand and only to a minor degree on any other molecular component.

C. Assignment of Al–ATP Spectra. Certain peak assignments of Al–ATP can be deduced by comparison with the model compounds. Thus the peaks upfield of the α–γ region and the β region can be ascribed to Al bound to γ- and β-phosphates, respectively.

The assignment of the resonances of the Al–ATP complexes on the basis of these model studies was confirmed by measuring the peak areas of the ^{31}P NMR spectra of Al–ATP mixtures, starting at high pH, because the resonances at basic pH were readily identifiable as peaks from uncomplexed ATP. In the following discussion, Al-bound peaks are designated with one or more ′. At pH 12 (Figure 3G), the ^{31}P NMR spectrum is nearly identical with ATP in the absence of aluminum, and therefore nearly all the ATP is dissociated from Al. At pH 8 (Figure 3E), the γ and β resonances are reduced and broad shoulders appear upfield of the α doublet and β triplet. The α doublet does not appear to be affected. The sum of the areas of the γ-phosphate doublet and the shoulder upfield of the α doublet (γ') is equal to one phosphate, within experimental error, at pH <11. The sum of the β triplet and the upfield shoulder (β') equals one phosphate. Peaks γ' and β' increase in amplitude with decreasing pH, while the amplitudes of the γ and β peaks decrease. At pH 7, the spectrum consists of only two broad resonances with an area ratio of 2:1 between downfield and upfield peaks. The upfield peak appears to be β', increased in intensity. The broad downfield peak appears to contain γ' and, slightly more downfield, the α resonance.

As these resonances are followed to still lower pH (Figure 3C), the peak containing γ' and α is somewhat broadened and two new peaks at −18 (β'') and −25 ppm (β''') appear with a concomitant decrease in β' intensity. The combined intensity of the β', β'', and β''' peaks remains constant, in line with all of these peaks originating from β-phosphate. At low pH the α and γ' peaks are clearly separated. Thus at pH 1 and 2 (Figure 3A), the five principal peaks are assigned to α, γ', β'', β, and β'''. The Al complex peaks, like the peaks due to uncomplexed phosphates, change position as a function of pH, as illustrated in Figure 6.

D. pH Dependence of Al–ATP Resonances. The interconversion between the different species indicated by these chemical shifts

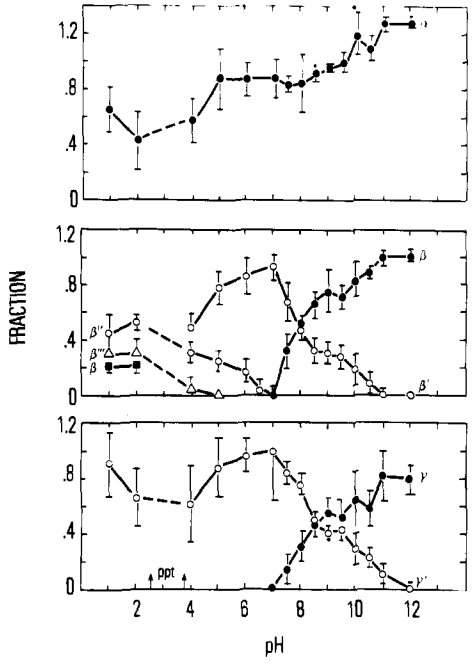

Figure 7. Relative intensities for resonance areas for 10 mM ATP–10 mM $AlCl_3$ solutions. Precipitation observed from pH ~2.5 to 3.8. See Discussion for identification of γ', β', β'', and β'''.

can be readily seen from the changes in intensity in the phosphate signals as a function of pH (Figure 7). For example, β''' represents ~33% of the total β-phosphate at pH 1 and <10% at pH 4. β'' represents about half the phosphate at acidic pH. An increase in β' between pH 4 and 6 is accompanied by a decrease in β''. Above pH 7 the intensity of the β' signal decreases, accompanied by an increase in the β (free) species. The β-phosphate resonance accounts for two-thirds of the β-phosphate by pH 9 and all the β-phosphate by pH 12. Although recovery of the β signal is full in the sense that no Al–complex signals are observed when the Al–ATP mixture reaches pH 12, the signal intensity for γ-phosphate at that pH is only ~85% of the intensity of the γ signal in uncomplexed ATP. No residual γ' signal is observed at pH 12 in Figure 7. Since it must exist, it presumably overlaps with the ATP α resonance in Figure 3G. The intensity of the α resonance is greater than one at this pH (Figure 7).

We have already noted (Figure 1E) that the ^{27}Al NMR results cannot be used to determine whether increased hydroxylation of the aluminum nucleus results in dissociation of Al from ATP. However, the ^{31}P NMR data summarized in Figure 7 indicate the degree of dissociation; for example, at pH 8, despite the absence of an ^{27}Al signal, about 70% of the aluminum remains bound to γ-phosphate.

Hydrogen-1 Spectra. To shed further light on the various Al–ATP complexes, we have employed ^1H NMR to examine the nonexchangeable downfield proton resonances.

A. Aluminum and ATP. The effect of Al on the ^1H NMR spectrum of ATP is rather unusual in that the Al–complex peaks can be clearly distinguished from the peaks due to uncomplexed ATP. Thus the slow-exchange phenomenon dominates the ^1H spectrum in the same way as the ^{27}Al and ^{31}P spectra already discussed.

The aluminum ion perturbs the ^1H NMR spectrum of ATP, like the spectra of the other nuclei, in a pH-dependent manner. At pH <3, there is a marked broadening and upfield shift of the H-8 resonance, but the H-2 and H-1′ resonances are not changed by the presence of aluminum (Figure 8, A and B). Above pH 4, the ^1H spectra consist of eight separate resonances that change in their relative areas as the pH is increased. The spectrum at pH 10 contains only resonances characteristic of unbound H-8, H-2, and H-1′ (Figure 8F).

At pH 8, a reduction of the Al uncomplexed proton peaks (f) is accompanied by the appearance of five additional resonances.

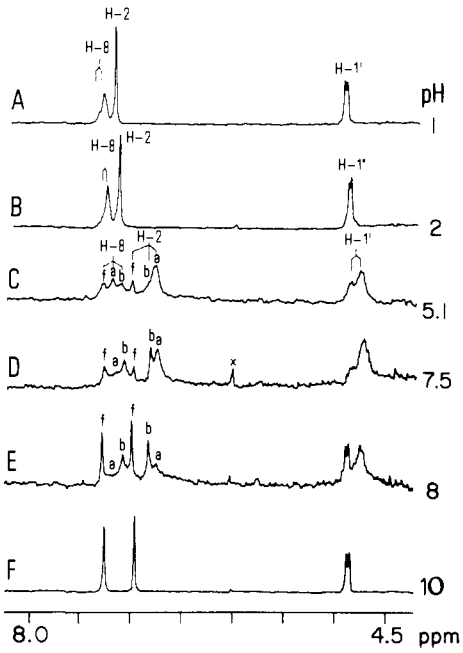

Figure 8. ^1H NMR spectra (200 MHz, 22 °C) of 10 mM $AlCl_3$–10 mM ATP in D_2O mixed at pH 1 (A), 2 (B), 5.1 (C), 7.5 (D), 8 (E), and 10 (F). Spectra were obtained with a spectral window of 3000 Hz, acquisition time 1.0 s, delay 10 s, line broadening 1 Hz, number of scans 80, internal 2-methyl-2-propanol reference. Vertical expansion of 40-fold for spectra C, D, and E. See Results for explanation of a, b, and f.

Two of these lie between the free H-8 and H-2; two can be found upfield of H-2; and the last is observed upfield of H-1′. At lower pH, although the H-1′ signal is broadened and the more upfield resonance increases in area, the total area of these two peaks remains constant. Likewise, although the six resonances in the ring-proton area change in relative intensity with decreased pH, the total area represents two protons and the area of the three more downfield peaks equals the area of the three more upfield peaks. Thus the areas of the various ^1H peaks provide clues for the assignment of the ^1H NMR peaks, in a manner analogous to the analysis of the ^{31}P data. We conclude that the H-8 and H-2 are observed in three different resonances while H-1′ is divided into two. Apparently, three chemical environments exist for the base protons, but two of these do not involve a detectable difference in the sugar resonance.

B. Aluminum and Adenosine. The effect of aluminum at low pH on the ^1H NMR spectrum of adenosine was studied in order to separate the effects of the binding of aluminum to the phosphate and the base moiety. Aluminum does not alter the ^1H spectra for 10 mM adenosine at pH ≤4.5 (Figure 9), in sharp contrast to the profound alterations observed for aluminum complexes with ATP (Figure 8). Thus the strong perturbations of the base protons of ATP by aluminum can involve binding of Al to base only in conjunction with the binding of Al to phosphate.

Discussion

Equilibria between Al and ATP. The NMR spectra of all three nuclei studied have in common the easy differentiation of peaks from complexed and uncomplexed forms because of the slow exchange between the aluminum and the ligands. Thus, the ^{27}Al spectra readily differentiate between hydrated aluminum and aluminum bound to ATP and other ligands, and the ^{31}P and ^1H spectra exhibit distinct peaks for Al-bound and free ligands.[13]

The resolution of the ^{27}Al peaks at low pH makes possible the calculation of the affinity of Al to ATP, with the not altogether expected finding that 97% of the Al is bound to ATP at pH 2, and the apparent stability constant at that pH is $1.1 \times 10^5\ M^{-1}$.

(13) Slow exchange has previously been observed for phosphorus and proton NMR spectra of Al(III), Be(II), and Ga(III) complexes with ATP at specific pH values: Bock, J.; Ash, D. *J. Inorg. Biochem.* **1980**, *13*, 105.

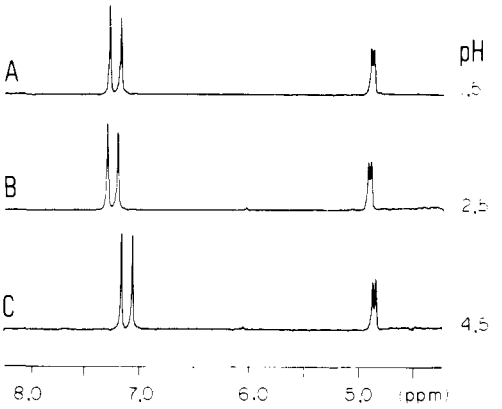

Figure 9. ^1H NMR spectra of 10 mM adenosine and 10 mM $AlCl_3$ at pH 1.5 (A), 2.5 (B), and 4.5 (C). NMR conditions as in Figure 8.

Al affinity to ATP remains very strong throughout the pH range, and 15% of the ATP is Al bound at pH 12.

The combination of results from the ^{31}P and ^1H spectra, in conjunction with the ^{27}Al results, show that Al forms a variety of complexes with ATP, that there is generally more than one complex present under any set of conditions, and that the equilibria between these complexes shift dramatically with pH. The pH effect is to be expected from a knowledge of the equilibria between Al species that exist in aqueous solutions that contain no other ligands except water and hydroxide ions.[5]

The superimposition of the peaks characteristic of free ATP on the spectrum of Al–ATP complex in the presence of only a slight excess of ATP indicates the predominance of 1:1 complexes. In most of the studies presented here, the employment of 1:1 solutions of Al and ATP made it unlikely that complexes containing a higher ratio of ligand to Al were present to complicate the equilibria.

Examination of the spectra of Al–ATP solutions observed at all pHs reveals that four different complexes with very different structures and consequently very different spectra exist in these solutions. The NMR spectra provide sufficient clues to furnish many of the structural characteristics of these complexes. We have put together all of these characteristics to define what we consider to be the most likely structures for these complexes. While we believe that the structures are based on a great deal of supportive evidence, we do not consider that our results can completely prove all aspects of these structures, and their depiction therefore involves a degree of speculation.

Comparison of Al–ATP Complexes with Al Complexes of Related Ligands. Binding of γ-Phosphate. The importance of the triphosphate group in the binding of Al to ATP becomes very clear from the following two considerations: (1) the ^1H spectrum of adenosine is quite unperturbed by Al (Figure 9) and (2) the ^{31}P spectra of Al–triphosphate (Figure 5) and Al–ATP (Figure 3) are remarkably similar, even when the pH transitions of the two systems are compared. Clearly the binding of Al to one end of the triphosphate molecule confers an ATP γ-P-like spectrum on that end and an ATP α-P-like spectrum on the other end. These results, along with the lack of a change in the chemical shift of α-ATP upon Al complexation, implicate γ-phosphate but not α-phosphate as binding sites.

Significance of ^{31}P Spectra. Binding of β-Phosphate. Binding of β-phosphate to aluminum produces three different perturbations on the ^{31}P NMR signals of phosphate compounds: (1) broadening, (2) upfield shifts for di- and triphosphates, and (3) downfield shifts for triphosphates only.

The broadening can be explained by scalar coupling of the quadrupolar aluminum ion to the phosphorus nucleus. Evidence comes from the fact that the ^2J value calculated from the ^{31}P line width has been found to be ~80 Hz, which can be compared to a previously determined value[10] of ~20 Hz for $Al[(MeO)_3PO]_6^{3+}$. Binding of Al(III) to ATP could give rise to diastereomers as reported for Co(III).[7e] Hence the broadening may also be due to the presence of unresolved diastereoisomers.

Table I

	NMR Nucleus		
	^{27}Al	^{31}P	^{1}H
complex I	−3.3 ppm	β''' upfield α broadened γ' upfield	unaffected
complex II	−3.1 ppm	β'' downfield α broadened γ' upfield	H-8 upfield
complex III	−0.9 ppm	β' upfield α broadened γ' upfield	H-8 upfield[a] H-2 upfield[a] H-1′ upfield[b]
complex IV	not detectable	γ' upfield	unaffected

[a] Split into three peaks. [b] Split into two peaks.

^{31}P chemical shift changes have been observed in response to alterations in geometry[14] and in dielectric constant of the solvent environment.[15] The variability of ^{31}P chemical shifts resulting from metal ion binding makes it difficult to interpret such results for any given metal complex,[16] but our comparison of related aluminum complexes has aided in the assignments of the peaks.

Aluminum binding to both di- and triphosphates is always accompanied by upfield shifts, and we therefore consider such shifts as indicative of direct binding of aluminum to phosphate. In fact, protonation of the ATP, like Al binding, produces a 6 ppm shift to higher field for γ-phosphates (Figure 6).

Downfield shifts are observed only with the central phosphate of triphosphates and not with diphosphates and must therefore be attributed to a phenomenon that can occur only with the former. In the following discussions, we relate upfield shifts to aluminum binding; when downfield shifts occur, we consider the possibility that they are caused by indirect effects that do not require direct Al binding, but we cannot rule out the possibility that direct Al binding can lead to such a shift.

β-Phosphate binding as indicated by the characteristic upfield shift is implicated in two of the complexes summarized in Table I. Another complex (II) exhibits the downfield shift and therefore may or may not involve β-phosphate binding. Table I contains a summary of all the NMR characteristics of the complexes produced between Al and ATP. We shall now analyze these characteristics to determine what structural features of the complexes they may reflect. We shall discuss the four complexes in the order in which they appear as the pH is raised.

The chemical shifts observed in the NMR spectra at pH 1 and 2 indicate the coexistance of two species, one of which decreases and the other increases in concentration with increasing pH. We call these species complex I and complex II, respectively.

Complex I exists only at very acid pH (1–2). The ^{31}P spectrum of this complex contains upfield shifts for β- and γ-phosphates (β''', γ') that indicate aluminum binding to the β- and γ-phosphates. The broadening and upfield shifts from the position at $Al(H_2O)_6^{3+}$ in the ^{27}Al spectrum of ATP confirms the binding of aluminum to phosphate. In the ^{1}H spectrum, the H-8 resonance of complex I is present as a shoulder that has not been shifted from its position in uncomplexed ATP. The essential features of complex I, therefore, are binding to γ- and β-phosphates and no other ligands; the other Al(III) coordination sites are presumably filled with water molecules, as shown in Chart I.

The concentration of this complex diminishes between pH 1 and 2 as that of complex II increases.

Complex II. This complex exists between pH 1 and 4. Its ^{31}P NMR characteristics are the downfield-shifted β'' signal and the upfield-shifted γ'. We conclude that the Al is bound to γ-phosphate, but we are uncertain about the coordination to β-phosphate. The ^{27}Al spectrum provides some evidence for a change from chelation to two phosphates in complex I to a monophosphate coordination in complex II; a downfield shift in the ^{27}Al peak is accompanied by an alteration in the β peak in the ^{31}P spectrum, which may be due to the displacement of a phosphate by a different ligand and the resulting decrease in the symmetry of coordination.

Chart I. Postulated Structure for Complex I

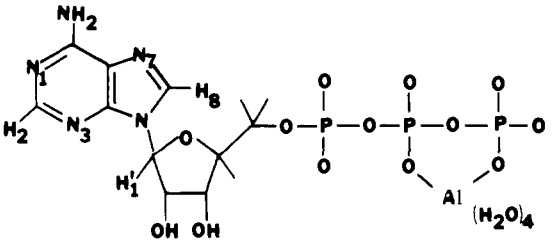

Chart II. Possible Structure for Complex II, Which Could Also Be Polymeric or Monomeric

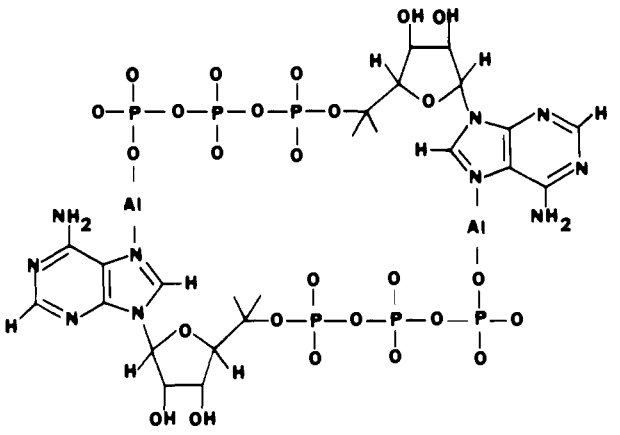

The ^{1}H NMR spectrum provides a reason for the possible lack of a β-phosphate–Al bond in Complex II. The selective upfield shift of H-8 without perturbation of H-2 or H-1′ indicates preferential binding of aluminum to N-7. Thus, it can be argued that in complex II the binding of N-7 of adenine can substitute for the β-phosphate binding observed in complex I. We have proposed a structure for complex II in Chart II that contains Al binding to N-7 and γ-phosphate only. We believe that the evidence favors a structure that does not include β-phosphate binding, although this evidence is weak and additional binding to β-phosphate is not ruled out.

Chart II also assumes binding of Al to N-7 of one ATP and γ-phosphate of another in either the dimeric form shown or a higher oligomeric form. This assumption is based on the formation of similar structures in other metal–nucleotide complexes.[17] However, our data are equally well explained by a macrochelate in which the N-7 and γ-phosphate of the same ATP molecule bind aluminum in a manner similar to structures proposed for ATP complexes with Co(II), Cu(II), and Mn(II).[18]

Complex III. This complex, which exists in the pH range 4–8, is characterized by upfield-shifted β- and γ-phosphate signals (β' and γ', respectively) in the ^{31}P spectrum, in accord with the binding of both β- and γ-phosphates to aluminum. Further evidence for such binding comes from the ^{27}Al spectrum, which exhibits a sharper signal for complex III than for complex II (35 vs. 61 Hz), and may indicate the greater Al(III) coordination symmetry consistent with the participation of two phosphates in the coordination.

An interesting feature of the NMR characteristics of what we call complex III is that the ^{1}H peaks in both the H-8 and the H-2

(14) (a) Gorenstein, D. G.; Kai, D. *Biochem. Biophys. Res. Commun.* **1975**, *65*, 1073. (b) Gorenstein, D. G. *J. Am. Chem. Soc.* **1975**, *97*, 898.
(15) Kearns, D. R.; Lerner, D. *J. Am. Chem. Soc.* **1980**, *102*, 7611.
(16) Jaffe, E. K.; Cohn, M. *Biochemistry* **1978**, *17*, 652.
(17) (a) Rifkind, J. M.; Eichhorn, G. L. *J. Am. Chem. Soc.* **1972**, *94*, 6526. (b) Berger, N. A.; Eichhorn, G. L. *Biochemistry* **1971**, *10*, 1847.
(18) (a) Wee, V. T.; Feldman, I.; Rose, P.; Gross, S. *J. Am. Chem. Soc.* **1974**, *96*, 103. (b) Torreilles, J.; Crastes de Paulet, A. *Biochimie* **1973**, *55*, 845. (c) Naumann, C. F.; Prijs, B.; Sigel, H. *Eur. J. Biochem.* **1974**, *41*, 209.

Chart III. Model for Stacked Structure Containing Different Types of Base Stacking—a Possible Configuration of Complex III

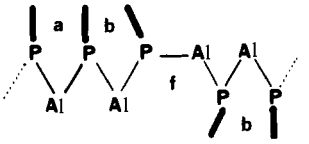

Chart IV. Postulated Structure for Complex IV

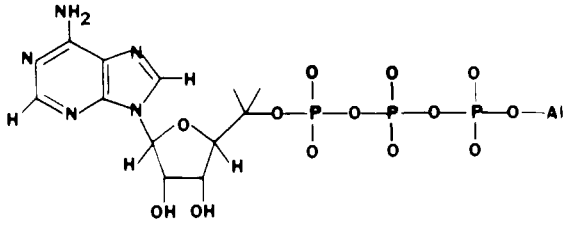

regions are split into three peaks in the region around neutral pH (two peaks can also be identified in the H-1′ region). The similarity of the splitting of the H-2 and the H-8 peaks, unlike the preferential effect on H-8 at lower pH, makes it unlikely that aluminum is bound to a specific base site as in complex II. Rather a general perturbation of the adenine ring by base stacking appears likely. Generally base-stacking interaction is accompanied by fast-exchange phenomena in NMR spectra;[19] however, the appearance of a slow exchange in this instance indicates that the base stacking is stabilized by another structural component, presumably the Al–phosphate bridging. The greater downfield shift of the ^{27}Al peak in complex III probably represents substitution of hydroxide for waters of hydration in a manner similar to that observed for carboxyl ligands.[8]

The split of the ^{1}H resonance into three peaks can be interpreted by the existence of three different complexes in this pH range, all with Al bound to β- and γ-phosphates but differentiated by different types of base stacking as indicated by peaks a and b (Figure 8); one complex (peaks f, Figure 8) would have no base stacking. Such an interpretation remains plausible. However, the lack of any change in the ^{31}P NMR in this pH region leads to an intriguing possibility; namely, that all three of these structures are really part of the same structure. Such a product would result from the formation of Al bridges between nucleotides. The bases then twist around the aluminum–phosphate axis in such a way that minimal stacking (f) alternates with two different types of stacking (a, b). The stacking sequence could be abfbafabfbaf, for example, (Chart III). We have obtained CD evidence that supports the persistence of such stacked structures when solutions employed for NMR experiments are diluted.

Complex IV. As the pH is increased above 7, the intensity of both the β' and γ' resonances in the ^{31}P NMR spectrum gradually decreases, but the γ' intensity is always higher than the β' intensity, in line with the continued binding of γ-phosphate during the release of β-phosphate. It therefore appears that a complex IV is produced in which only γ-phosphate remains bound. Such a structure is supported by ^{27}Al spectra, which become increasingly broad with increasing pH, indicating a reduction in symmetry, probably caused by the replacement of the β-phosphate in the ligand field by one or more hydroxides. Although nearly 50% of the ATP γ-phosphate remains complexed to Al at pH 10, the ^{1}H spectrum is indistinguishable from that of native ATP, thus demonstrating the insensitivity of the nucleoside protons to γ-phosphate binding. We assume the structure of complex IV shown in Chart IV.

We have noted that aluminum displays a very strong affinity for ATP phosphate throughout the pH range and is 79% bound at pH 1 and 15% at pH 12. Once free γ-phosphate appears in the ^{31}P NMR spectrum, ATP is apparently free to participate in enzyme reactions; the appearance of uncomplexed ATP parallels the restoration of hexokinase[4a,d] and RNA polymerase[20] activities.

Table II. Exchange Rates[a] between the Various Aluminum Complexes

exchanging complexes	NMR nucleus observed	spectral appearance	exchange rate limits,[b] s^{-1}	actual rate, s^{-1}
$[Al(H_2O)_6]^{3+}$ ↔ complex I	^{27}Al	slow	<u><1100</u>	
	^{31}P, γ	slow	<2000	
	^{31}P, β''	slow	<1400	
complex I ↔ complex II	^{27}Al	fast	>60	~65
	^{31}P, β''	slow	<3000	
	^{1}H, H_8	slow	<70	
complex II ↔ complex III	^{27}Al	fast	>700	~1000
	^{31}P, β'	slow	<1300	
complex III ↔ complex IV	^{1}H, H_1'	slow	<u><140</u>	
	^{1}H, H_2(a)[c]	slow	<290	
	^{1}H, H_2(b)	slow	<220	
	^{1}H, H_8(a)	slow	<250	
	^{1}H, H_8(b)	slow	<160	
complex IIIa ↔ complex IIIb	^{1}H, H_2	slow	<u><90</u>	
	^{1}H, H_8	slow	<90	

[a] In those cases where separate NMR peaks are observed for the chemical species in equilibrium (slow exchange), the upper limit for the exchange rate can be calculated[21,22] from the frequency difference of the corresponding peaks. In instances when single peaks are observed in frequency positions that are the weighted average of the positions of the species in equilibrium (fast exchange), a lower limit for the exchange rate is derived by measuring the chemical shift difference in the position of the peak at two different pH values. Those pH values are chosen such that one of the two exchanging species predominates. Since fast exchange has been observed, the actual rate of exchange is obviously greater than the limiting chemical shift difference obtained in the above manner. Therefore the exchange rates calculated from fast exchange data are only a lower limit to the actual rates. [b] Calculated, with lowest observed upper limit underlined. [c] (a) and (b) refer to notation used in Figure 8.

Cleland et al.[7] have put the Cr(III) and Co(III) complexes of ATP and derivatives to extensive use in the study of enzyme structure and function. Although there are some similarities between the Al(III)–ATP complexes and the ATP complexes of Cr(III) and Co(III) studied by Cleland and co-workers, the complexes also have quite different properties, as might be expected from the availability of d electrons for bonding in Co(III) and Cr(III) but not in Al(III). Thus, whereas Co(III) induces downfield shifts (7–14 ppm) in ^{31}P resonances,[7e] Al(III) produces upfield shifts of 3–5 ppm (with the exception of the central of three linked phosphates). All three metals bind to both phosphates in pyrophosphate and ADP.[7a,e,i] Frequently, however, fewer phosphate groups are bound in the case of Al(III). Thus, we find monodentate and bidentate phosphate coordination in Al(III) complexes of ATP and bidentate coordination in Al(III)–triphosphate, but Cleland et al. report bidentate and tridentate phosphate coordination of triphosphate and ATP to Co(III)[7e] and Cr(III).[7a,i] To some extent, differences in reaction conditions could account for these differences, but so far we have found no evidence for tridentate phosphate binding to Al(III) under a wide range of conditions. At this time there is no evidence of Co(III) or Cr(III) binding to adenosine or promoting base stacking, as there is for Al(III)–ATP complexes II and III, respectively.

Some similarities that can be cited are the reduction of the secondary pH of γ-phosphate in both Al(III)- and Cr(III)–ATP to ~2[7a] and the similarity in structure of similarly liganded complexes, which arises of course from the limitations of the octahedral geometry.

Kinetics of Chemical Exchange. NMR spectra can yield information about kinetics as well as about equilibria and struc-

(19) Patel, D. *Biochemistry* **1975**, *14*, 3984.

(20) Crapper-McLachlan, D. R.; Galen, H.; Farnell, B.; DeBoni, U.; Karlik, S. J.; Eichhorn, G. L. In "Metal Ions in Health and Disease"; Sarkar, B., Ed.; Raven Press: New York, in press.

ture.[21,22] In Table II the rates of exchange between the various complexes discussed in this paper are compiled. These rates are based on the experimental data presented in Figures 1, 3, and 8. Most frequently upper limits only of exchange rates can be calculated. Whenever the different observed nuclei give different upper limits, the lowest of these is the closest to the actual rate. Therefore, the hydrated aluminum exchanges with complex I at a rate slower than 1100 s^{-1}, and complexes III and IV have a rate between them smaller than 130 s^{-1}. Likewise, structures a and b within complex III exchange at a rate slower than 90 s^{-1}. In two cases, between complex I and complex II and also between complex II and complex III, both a lower and an upper limit are available. The ability, in these cases, to obtain both limits is due to the fortunate coincidence of two different NMR nuclei having chemical shift differences such that one happens to be in slow and the other in fast exchange relative to their reference rates. Therefore, the actual chemical exchange rates become revealed due to this bracketing. These are ~65 s^{-1} for the exchange between complexes I and II and 1000 s^{-1} for complexes II and III.

(21) Pople, J.; Schneider, W. G.; Bernstein, H. J. "High Resolution Nuclear Magnetic Resonance"; McGraw Hill: New York, 1959.
(22) Swift, T. J.; Connick, R. E. *J. Chem. Phys.* **1962**, *37*, 307.

Acknowledgment. We thank Dr. R. P. Pillai for a critical reading of the manuscript and Dr. Peter Roller for letting us use his NMR instrument while ours was out of order.

Simulation of Reaction Pathways in Enzymatic and Nonenzymatic Hydrolysis of *p*-Nitrophenyldeoxythymidine Diphosphate

Joan A. Deiters[1a] and Robert R. Holmes*[1b]

Contribution from the Departments of Chemistry, University of Massachusetts, Amherst, Massachusetts 01003, and Vassar College, Poughkeepsie, New York 12601.
Received May 10, 1982

Abstract: A computer model, based on a molecular mechanics approach, is developed for the hydrolysis of the substrate *p*-nitrophenyldeoxythymidine diphosphate, *p*-NO_2Ph-pdTp, in the enzyme system Ca^{2+}–staphylococcal nuclease. The model is based on X-ray data (1.5-Å resolution) for the enzyme substrate system Ca^{2+}–staphylococcal nuclease–pdTp, where pdTp represents deoxythymidine diphosphate. Calcium–oxygen interactions and hydrogen bonding are included in the model to mimic enzyme–substrate interaction. The energy profiles of two hydrolysis pathways are investigated: path 1, an attack at phosphorus in line with OR where R = *p*-NO_2Ph, leads to the products observed experimentally in nonenzymatic hydrolysis; path 2, attack at phosphorus in line with OR′ where R′ = deoxythymidine 3′-phosphate, leads to the products observed in enzymatic hydrolysis. The results of the calculation, done under constraints similar to those used for 2.0-Å data, show that in the enzymatic system path 1 is of higher energy unless extensive atomic rearrangement occurs. The higher energy of path 1 results from the fact that attack in line with OR, where R = *p*-NO_2Ph, is blocked by a nitrogen atom of Arg-35. The results calculated from the enzymatic system are compared also with the earlier calculation on nonenzymatic hydrolysis of *p*-NO_2Ph-pdTp.

Introduction

Possible mechanisms for the action of the enzyme staphylococcal nuclease–Ca^{2+} in phosphate hydrolysis have been proposed[2,3] based on experimental data giving structural information for the active site. These data have been based on NMR investigations utilizing paramagnetic probes[4] and single-crystal X-ray diffraction studies.[3b,5,6] In a previous paper[7] using atomic coordinates from X-ray diffraction studies,[5,8,9] the methods of molecular mechanics were applied to give a computer simulation of the energy profile for enzymatic and nonenzymatic hydrolysis of the substrate *p*-nitrophenyl-pdTp where pdTp is deoxythymidine diphosphate. The initial conformation of the substrate *p*-nitrophenyl-pdTp in the active site of the enzyme, staphylococcal nuclease–Ca^{2+}, was obtained by modifying the X-ray coordinates of 2.0-Å resolution for the inhibitor–enzyme complex, pdTp–Ca^{2+}–staphylococcal nuclease. When a further refinement of the X-ray data to 1.5-Å resolution showed that there was considerable change in the active site,[3b] particularly in the region immediately surrounding the calcium ion, we wished to see how these changes in atomic coordinates affected the energy profile of possible hydrolysis reaction pathways and also whether or not there were high-energy barriers along the reaction pathway proposed by Cotton and Hazen[3b] based on X-ray data of 1.5-Å resolution. In this present work, the atomic coordinates of 1.5-Å resolution, obtained from the inhibitor–enzyme complex pdTp–Ca^{2+}–staphylococcal nuclease, are used and modified to obtain a minimum energy conformation for the active substrate *p*-nitrophenyl-pdTp in an enzymatic environment. The energy profile of two possible reaction pathways was calculated and compared with earlier results based on 2.0-Å data[7] and

(1) (a) Vassar College. (b) University of Massachusetts.
(2) Anfinsen, C. B.; Cuatrecasas, P.; Taniuchi, H. "The Enzymes", 3rd ed.; Boyer, P. D., Ed.; Academic Press: New York, 1971; Vol. IV, pp 177–204.
(3) (a) Cotton, F. A.; Day, V. W.; Hazen, E. E., Jr.; Larsen, S. *J. Am. Chem. Soc.* **1973**, *95*, 4834. (b) Cotton, F. A.; Hazen, E. E., Jr.; Legg, M. J. *Proc. Natl. Acad. Sci. U.S.A.* **1979**, *76*, 2551.
(4) Furie, B.; Griffen, J. H.; Feldmann, R. J.; Sokoloski, E. A.; Schechter, A. N. *Proc. Natl. Acad. Sci. U.S.A.* **1974**, *71*, 2833.
(5) Arnone, A.; Bier, C. J.; Cotton, F. A.; Day, V. W.; Hazen, E. E., Jr.; Richardson, D. C.; Richardson, J. S.; Yonath, A. *J. Biol. Chem.* **1971**, *246*, 2302.
(6) Arnone, A.; Bier, C. J.; Cotton, F. A.; Hazen, E. E., Jr.; Richardson, D. C.; Richardson, J. S. *Proc. Natl. Acad. Sci. U.S.A.* **1969**, *64*, 420.
(7) Deiters, J. A.; Gallucci, J. C.; Holmes, R. R. *J. Am. Chem. Soc.* **1982**, *104*, 5457.
(8) Trueblood, K. N.; Horn, P.; Luzzati, V. *Acta Crystallogr., Sect. B* **1961**, *14*, 965.
(9) Young, D. W.; Tollin, P.; Wilson, H. R. *Acta Crystallogr., Sect. B* **1969**, *25*, 1423.

0002-7863/83/1505-0609$01.50/0